The association between subcortical and cortical fMRI and lifetime noise exposure in listeners with normal hearing thresholds

Rebecca S Dewey[a,b,c], Susan T Francis[a], Hannah Guest[d], Garreth Prendergast[d], Rebecca E Millman[d,e], Christopher J Plack[d,e,f], Deborah A Hall[b,c,g]

Affiliations

a. Sir Peter Mansfield Imaging Centre, School of Physics and Astronomy, University of Nottingham, NG7 2RD, UK.

b. National Institute for Health Research (NIHR) Nottingham Biomedical Research Centre, Nottingham, NG1 5DU, UK.

c. Hearing Sciences, Division of Clinical Neuroscience, School of Medicine, University of Nottingham, NG7 2UH, UK.

d. Manchester Centre for Audiology and Deafness (ManCAD), University of Manchester, Manchester Academic Health Science Centre, M13 9PL, UK.

e. National Institute for Health Research (NIHR) Manchester Biomedical Research Centre, Central Manchester University Hospitals NHS Foundation Trust, Manchester, M13 9WL, UK.

f. Department of Psychology, Lancaster University, LA1 4YF, UK.

g. University of Nottingham Malaysia, Jalan Broga, 43500 Semeniyh, Selangor Darul Ehsan, Malaysia.

Author information

Dewey: Rebecca Susan Dewey; Sir Peter Mansfield Imaging Centre, School of Physics and Astronomy, University of Nottingham, UK. NG1 5DU; Rebecca.dewey@nottingham.ac.uk

Francis: Susan T Francis; Sir Peter Mansfield Imaging Centre, School of Physics and Astronomy, University of Nottingham, UK. NG7 2RD; susan.francis@nottingham.ac.uk

Guest: Hannah Guest; Manchester Centre for Audiology and Deafness (ManCAD), University of Manchester, UK. M13 9PL; hannah.guest@manchester.ac.uk

Prendergast: Garreth Prendergast; Manchester Centre for Audiology and Deafness (ManCAD), University of Manchester, UK. M13 9PL; garreth.prendergast@manchester.ac.uk

Millman: Rebecca E Millman; Manchester Centre for Audiology and Deafness (ManCAD), University of Manchester, Manchester, UK. M13 9PL; Rebecca.millman@manchester.ac.uk

Plack: Christopher John Plack; Manchester Centre for Audiology and Deafness (ManCAD), University of Manchester, UK. M13 9PL; chris.plack@manchester.ac.uk

Hall: Deborah Ann Hall; University of Nottingham Malaysia, Jalan Broga, 43500 Semeniyh, Selangor Darul Ehsan, Malaysia; deborah.hall@nottingham.edu.my

Corresponding author:

Rebecca Susan Dewey; National Institute for Health Research (NIHR) Nottingham Biomedical Research Centre, Nottingham, UK. NG1 5DU; +441158232638; Rebecca.dewey@nottingham.ac.uk

Susan T Francis; Sir Peter Mansfield Imaging Centre, School of Physics and Astronomy, University of Nottingham, UK. NG7 2RD; +44115 846 6518; susan.francis@nottingham.ac.uk

Data and code availability statement

We are willing and able to provide raw and/or processed data and Matlab scripts on request.

Abstract

In animal models, exposure to high noise levels can cause permanent damage to hair-cell synapses (cochlear synaptopathy) for high-threshold auditory nerve fibers without affecting sensitivity to quiet sounds. This has been confirmed in several mammalian species, but the hypothesis that lifetime noise exposure affects auditory function in humans with normal audiometric thresholds remains unconfirmed and current evidence from human electrophysiology is contradictory. Here we report the auditory brainstem response (ABR), and both transient (stimulus onset and offset) and sustained functional magnetic resonance imaging (fMRI) responses throughout the human central auditory pathway across lifetime noise exposure. Healthy young individuals aged 25-40 years were recruited into high (n = 32) and low (n = 30) lifetime noise exposure groups, stratified for age, and balanced for audiometric threshold up to 16 kHz. fMRI demonstrated robust broadband noise-related activity throughout the auditory pathway (cochlear nucleus, superior olivary complex, nucleus of the lateral lemniscus, inferior colliculus, medial geniculate body and auditory cortex). fMRI responses in the auditory pathway to broadband noise onset were significantly enhanced in the high noise exposure group relative to the low exposure group, differences in sustained fMRI responses did not reach significance, and no significant group differences were found in the click-evoked ABR. Exploratory analyses found no significant relationships between the neural responses and self-reported tinnitus or

reduced sound-level tolerance (symptoms associated with synaptopathy). In summary, although a small effect, these fMRI results suggest that lifetime noise exposure may be associated with central hyperactivity in young adults with normal hearing thresholds.

Keywords

Noise induced hearing loss, functional magnetic resonance imaging; auditory pathways; auditory brainstem response

Abbreviations

ABR = auditory brainstem response; CN = cochlear nucleus; CSF = cerebrospinal fluid EEG = electroencephalography; EPI = echo planar imaging; fMRI = functional magnetic resonance imaging; GE = gradient echo; HL = hearing level, IC = inferior colliculus; MGB = medial geniculate body; MNI = Montreal Neurological Institute; MPRAGE = magnetization prepared rapid acquisition gradient echo; MRI = magnetic resonance imaging; SENSE = sensitivity encoding; SPL = sound pressure level; TE = echo time; TR = repetition time; TSE = turbo spin echo

Acknowledgments

1. Introduction

Noise exposure is the main cause of preventable hearing loss (World Health Organization, 1997). Cochlear damage from noise exposure can lead to increased hearing thresholds, tinnitus (perception of sound with no external source) and diminished sound-level tolerance (Sliwinska-Kowalska and Zaborowski, 2017; Di Stadio et al., 2018). Animals exposed to high sound levels exhibit temporary threshold shifts, which may be accompanied by permanent loss of synapses between inner hair cells and auditory nerve fibers and permanent reduction of wave I of the electrophysiological auditory brainstem response (ABR) (Kujawa and Liberman, 2009). This cochlear synaptopathy may preferentially affect high-threshold auditory nerve fibers (Furman et al., 2013), i.e. fibers thought to encode acoustic information at medium-to-high levels and in background noise (Young and Barta, 1986). Importantly, cochlear synaptopathy can remain "hidden" because the synaptic loss can occur without a permanent hearing threshold shift. Synaptopathy has now been evidenced in mice, rats, guinea pigs, gerbils, chinchillas, and even macaques (Hickox et al., 2017), suggesting a common mechanism in mammals.

It has been hypothesized previously that damage to neural structures precedes hair cell loss, but that this damage may not be revealed by pure tone audiometric thresholds (Zhao and Stephens, 2007). The lack of any diagnostic assessment that is sufficiently sensitive and yet adequately specific has hindered the reliable demonstration of cochlear synaptopathy in humans. Current evidence is mixed. Some studies suggest adults with a history of noise exposure, but with normal hearing as measured by pure-tone audiometry, experience problems with sound discrimination and in particular understanding speech in noise. Noise-exposed workers demonstrated worse speech recognition in multi-talker babble compared to controls (Kumar et al., 2012), and high-noise-risk college students scored lower on word recognition in noise than low-noise-risk counterparts (Liberman et al., 2016). However, other studies found no evidence of a link between noise exposure and speech perception deficits for listeners with normal audiometric thresholds (Grose et al., 2017; Prendergast et al., 2017b; Yeend et al., 2017; Guest et al., 2018a). It may be the case that compensatory behavioral strategies protect performance, especially in high functioning individuals with a normal clinical audiogram, but that nevertheless the effect of synaptopathy in humans might be detected by measurements

27   of physiological function within the central auditory system (Kobel et al., 2017). From animal data, symptoms

28   such as tinnitus and reduced sound-level tolerance in the presence of normal thresholds can potentially be

29   explained by the central gain hypothesis, which states that reduced peripheral auditory input following

30   cochlear damage (for example, synaptopathy) produces a compensatory increase in spontaneous and sound-

31   related activity throughout the ascending auditory pathway (see Auerbach et al., 2014 for a review).

32   Non-invasive imaging can be used to investigate such pathophysiological mechanisms. ABR waves I-II reflect

33   peripheral auditory function, whilst waves III-V reflect central auditory function. Some studies report

34   associations between ABR wave I amplitude and estimates of noise exposure (Stamper and Johnson, 2015b;

35   Bramhall et al., 2017; Valderrama et al., 2018), whilst others show no discernible relationship between ABR

36   wave I and noise exposure (Fulbright et al., 2017; Grinn et al., 2017; Prendergast et al., 2017a). Some studies

37   have shown that participants with tinnitus have a reduced wave I of the ABR but normal (Schaette and

38   McAlpine, 2011; Gu et al., 2012; Bramhall, 2019) wave V. An increased wave V/I ratio is indicative of central

39   gain enhancement. The argument is that reduced peripheral input due to synaptopathy results in enhanced

40   central neural gain, leading to the perception of tinnitus (Schaette and McAlpine, 2011). However, other

41   studies show no association between tinnitus and ABR wave amplitudes (Guest et al., 2017; Shim et al.,

42   2017).

43   To date, no study has examined the effects of noise exposure using functional magnetic resonance imaging

44   (fMRI). However, physiological correlates of tinnitus and sound-level tolerance have been detected within

45   subcortical structures. Notably, Gu et al. (2010) observed an increased sustained fMRI response in the

46   inferior colliculus (IC) and Medial Geniculate Body (MGB) to continuous broadband noise as a function of

47   decreased sound-level tolerance, which they interpreted as central gain enhancement. It is known that

48   subcortical structures (such as the IC) respond to continuous sounds with a sustained fMRI response, while

49   the response in primary auditory cortex is predominantly transient with phasic peaks immediately after

50   onset and offset (Harms and Melcher, 2002). Therefore, sustained and phasic responses at different

51   positions in the auditory pathway might be differentially sensitive to noise exposure.

52   This article reports the first investigation of cumulative lifetime noise exposure on ascending auditory

53   pathway function in audiometrically normal adults, as measured by the sustained and transient fMRI

54   response and associated ABR in the same participants. Our primary hypothesis, informed by (Gu et al., 2010)

55   and as pre-registered in Dewey et al. (2018a) was that higher lifetime noise exposure would lead to

56   increased fMRI and ABR responses in central auditory regions compared to lower noise exposure, consistent

57   with central gain enhancement (Gu et al., 2010; Gu et al., 2012; Auerbach et al., 2014) as a consequence of
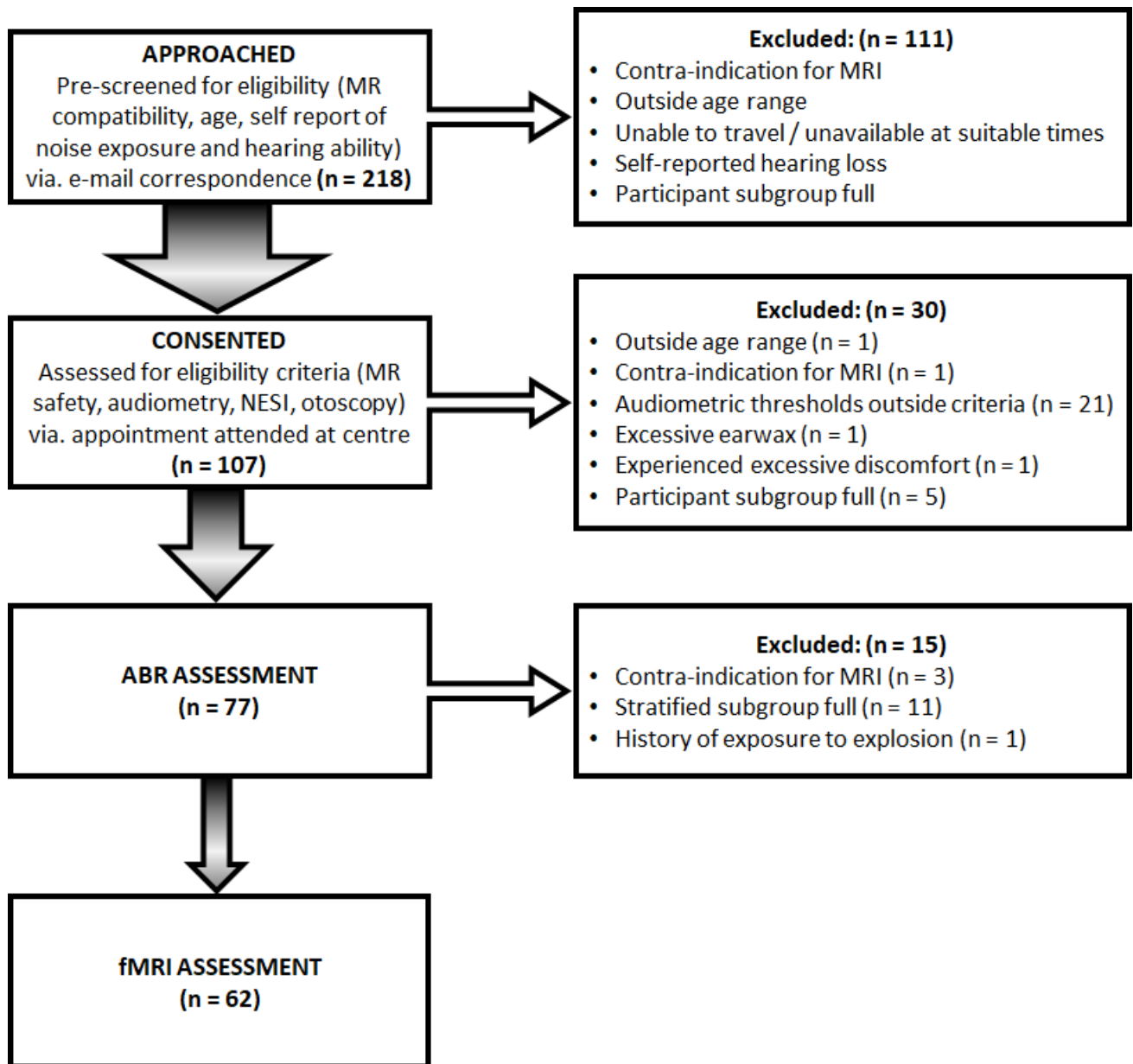
58   cochlear synaptopathy.

59

60   ## 2. Materials and Methods

61   A protocol for this study has been published in (Dewey et al., 2018a), as recommended by The Organization

62   for Human Brain Mapping (OHBM) Committee on Best Practice in Data Analysis and Sharing (COBIDAS;

63   Nichols et al., 2017).

64

65   **2.1 Participants**


```
┌─────────────────────────────┐        ┌──────────────────────────────────────────────┐
│         APPROACHED          │        │ Excluded: (n = 111)                            │
│ Pre-screened for eligibility│───────▶│ • Contra-indication for MRI                    │
│  (MR compatibility, age,    │        │ • Outside age range                            │
│  self report of noise       │        │ • Unable to travel / unavailable at suitable   │
│  exposure and hearing       │        │   times                                        │
│  ability) via. e-mail       │        │ • Self-reported hearing loss                   │
│  correspondence (n = 218)   │        │ • Participant subgroup full                    │
└─────────────────────────────┘        └──────────────────────────────────────────────┘

┌─────────────────────────────┐        ┌──────────────────────────────────────────────┐
│         CONSENTED           │        │ Excluded: (n = 30)                             │
│ Assessed for eligibility    │        │ • Outside age range (n = 1)                    │
│ criteria (MR safety,        │───────▶│ • Contra-indication for MRI (n = 1)            │
│ audiometry, NESI, otoscopy) │        │ • Audiometric thresholds outside criteria      │
│ via. appointment attended   │        │   (n = 21)                                     │
│ at centre (n = 107)         │        │ • Excessive earwax (n = 1)                     │
│                             │        │ • Experienced excessive discomfort (n = 1)     │
│                             │        │ • Participant subgroup full (n = 5)            │
└─────────────────────────────┘        └──────────────────────────────────────────────┘

┌─────────────────────────────┐        ┌──────────────────────────────────────────────┐
│       ABR ASSESSMENT        │        │ Excluded: (n = 15)                             │
│          (n = 77)           │───────▶│ • Contra-indication for MRI (n = 3)            │
│                             │        │ • Stratified subgroup full (n = 11)            │
│                             │        │ • History of exposure to explosion (n = 1)     │
└─────────────────────────────┘        └──────────────────────────────────────────────┘

┌─────────────────────────────┐
│       fMRI ASSESSMENT       │
│          (n = 62)           │
└─────────────────────────────┘
```

66

67   **Figure 1**: Flow chart showing participant recruitment through the study, detailing the number of participants

68   at each stage and reasons for their exclusion. Contraindications for MRI (n=3) identified after the eligibility

69   pre-screening stage were due to reasons that were revealed at a subsequent study visit; this included an

70   implant that had previously been thought to be MR compatible, and feelings of claustrophobia prior to the

71   appointment or whilst in the MR scanner.

72

73 Experimental procedures conformed to the World Medical Association's Declaration of Helsinki and were

74 approved by the University of Nottingham School of Medicine Research Ethics Committee (reference:

75 B/1207/2016). Participants aged 25 to 40 years, and with self-reported normal hearing, were recruited by

76 advertisment across the University, social media and online message boards. A sample size of 60 participants

77 was pre-defined to differentiate fMRI-related activity between noise exposure groups (n = 30 per group),

78 with 80% power (Dewey et al., 2018a). Figure 1 shows the recruitment of participants through the study and

79 reasons for exclusion. In total, 107 individuals were consented, and 62 met the eligibility criteria for both

80 fMRI and ABR assessments. Key inclusion criteria were normal hearing as defined by hearing thresholds in

81 each ear ≤ 20 dB HL between 0.5 and 8 kHz and absence of any otological condition as screened by otoscopy

82 and tympanometry. Audiometric thresholds were assessed in a sound-proofed booth using a bespoke

83 calibrated system as described in the protocol (Dewey et al., 2018a). Stimuli were presented using an M-

84 Audio M-Track Quad external sound card (M-Audio, Cumberland, Rhode Island, USA) over Sennheiser

85 HDA300 audiometric headphones suitable for high-frequency audiometry (Sennheiser electronic GmbH &

86 Co. KG, Wedemark, Germany). Stimuli were generated using in-house software written in Matlab (version

87 2016a, The MathWorks Inc., Natick, Massachusetts). Audiometry was performed using a two-interval, two-

88 alternative forced choice visually cued adaptive paradigm with a two-down one-up rule and a step size of 2

89 dB. The adaptive procedure was stopped after 12 reversals, and the geometric mean of the signal level at

90 the last eight reversals was computed. This paradigm was used to establish monaural thresholds, in the left

91 ear, followed by the right ear, at frequencies of 0.25, 0.5, 1.0, 2.0, 3.0, 4.0, 6.0, 8.0, 12.0, and 16.0 kHz.

92 Stimuli used at frequencies 250 Hz to 8 kHz were sinusoidal pure tones. Stimuli used at frequencies 12 kHz

93 and 16 kHz were half-octave narrowband noise, to minimize the influence of ear canal resonances and

94 threshold microstructure on measured thresholds. Any participants reporting lifetime noise exposure to

95 heavy weapon firing or explosions were excluded since under these circumstances noise exposure cannot be

96 reliably estimated (Guest et al., 2018c).

97 Group allocation was based on an estimate of lifetime noise exposure obtained using a beta version of the

98 Noise Exposure Structured Interview (NESI); a comprehensive structured interview which evaluates

recreational, occupational/educational, and firearm noise exposure (Guest et al., 2018c). The data collection

method in the NESI uses a calendar method which is a widely accepted instrument for enhancing

autobiographical recall by providing the respondent with event cues (Glasner and van der Vaart, 2009). In

particular, the NESI "provides fields for recording the timing of each exposure period and advises that any

contemporaneous life milestones (e.g., graduation or change of workplace) be noted to assist recall" (Guest

et al., 2018c, page 4). The NESI has been shown to have sensitivity in the separation of individuals with and

without tinnitus, based on noise exposure (Guest et al., 2017), and using robust estimates of noise level

(Ferguson et al., 2019), has been shown to reliably provide a coarse estimate of lifetime exposure (Guest et

al., 2018b). Further, the variance associated with NESI across participants with a range of lifetime noise

exposures is large compared to the error in the estimate of a given individual's noise exposure (Prendergast

et al., 2017b). The cut-off between 'high' and 'low' noise exposure was pre-specified at 15 units of lifetime

noise exposure, equivalent to 85 dB(A) across a full 50-year working lifetime (8 hours a day, 5 days a week,

48 weeks a year; National Institute for Occupational Safety and Health, 1998). Noise exposure groups were

balanced using age as a stratification variable (25-27, 28-30, 31-33, 34-36 and 37-40 years) (Dewey et al.,

2018a), but were chosen to not be balanced for sex since there is no specific hypothesis regarding auditory

fMRI responses and sex, thus avoiding issues with an already complex recruitment task (Figure 1). The

Tinnitus and Hearing Survey (THS, Henry, 2015) was used to assess self-reported tinnitus, hearing problems

and sound-level tolerance. The presence of tinnitus, hearing problems or reduced sound-level tolerance was

defined by a non-zero score (1-4) on any item in the corresponding subscale. Tinnitus intrusiveness was

assessed using the intrusiveness subscale of the Tinnitus Functional Index (TFI, Meikle et al., 2012).

2.2 Procedure overview

The study consisted of two sessions on separate days. In the first session, participants completed a

comprehensive structured interview to estimate lifetime noise exposure and underwent click-evoked ABR

testing. In a second session, participants underwent fMRI while listening to a broadband noise stimulus

designed to engage cortical and subcortical brain regions throughout the central auditory pathway.

125

2.3 Lifetime noise exposure

127 The NESI systematically assesses lifetime noise exposure from (1) recreational and (2) occupational and

128 educational noise. For each setting, participants were asked to identify activities they engage in that involve

129 being in an environment estimated to exceed 80 dB(A). The NESI prompts respondents to consider activities

130 experienced across different periods of the lifespan and to use life events as points of reference to improve

131 the quality of recall (Guest et al., 2018c). For each activity, participants were asked to estimate the level of

132 exposure using a vocal effort scale comprising six levels ranging from "raised voice" (87 dB(A)) to "shouting

133 close to listener's ear" (110 dB(A)) and to estimate the duration for which they were in that

134 environment/engaging in that activity, breaking this down into number of years, number of weeks per year,

135 number of days per week and number of hours per day. For each, participants were asked to recall whether

136 ear protection was used, what type, and the proportion of time for which that ear protection was effective.

137 Total lifetime noise exposure was calculated for each activity using Equation 1 (Lutman et al., 2008).

$$noise\ exposure = \frac{Y \times W \times D \times H}{2080} \times \left[P \times 10^{\frac{L-A-90}{10}} + (1-P) \times 10^{\frac{L-90}{10}} \right] \qquad (1)$$

138 where Y = number of years of exposure, W = number of weeks per year of exposure, D = number of days per

139 week of exposure, H = number of hours per day of exposure, L = estimated level of exposure in dB (A), A =

140 attenuation of hearing protective equipment (dB), and P = proportion of time protective equipment worn

141 (between 0 and 1). Units for all activities were calculated and summed to provide each participant's total

142 lifetime noise exposure, a measure linearly related to total energy of exposure above 80 dB(A). One unit of

143 noise exposure is equivalent to a working year (8 hours a day, 5 days a week, 52 weeks a year = 2080 hours)

144 of exposure to 90 dB(A).

145

2.4 fMRI assessment

fMRI was used to assess sound-related responses to broadband noise in brain regions of the ascending auditory pathway comprising the Cochlear Nucleus (CN), Superior Olivary Complex (SOC), Nucleus of the Lateral Lemniscus (NLL), Inferior Colliculus (IC), Medial Geniculate Body (MGB), and auditory cortex.

2.4.1 Stimuli

In-scanner communication, auditory stimulation and ear protection were delivered using an OptoActive Active Noise Cancellation Headphones system (Optoacoustics Ltd., Moshav Mazor, Israel) providing passive attenuation of 24 dB. The fMRI task comprised passive listening to a continuous steady-state broadband noise, filtered using a first-order Butterworth filter between 1.4 and 4.1 kHz, and presented at 85 dB SPL. Following an initial rest period of 64 s, broadband noise was presented for a 24-s 'on epoch' followed by 42-s 'off-epoch' in a block design. Following an initial 16-s learning period in the first fMRI timeseries, the active noise cancellation reduced the effective scanner sound level to approximately 70 dB SPL (accounting for both passive and active attenuation). This was achieved predominantly by attenuating the fundamental frequencies of the scanner noise, which can be attributed to the readout gradients in the EPI pulse sequence at 1.3 kHz and a mechanical resonance centered around 400 Hz, ensuring that the sound stimulus was clearly audible. During the entire 40-minute fMRI study, participants were instructed to attend to a fixation cross presented on a 32" BOLDscreen with a 1920 × 1080 widescreen LCD display (Cambridge Research Systems Ltd., Rochester, UK) positioned behind the scanner and viewed using a mirror attached to the head coil approximately 10 cm from the face.

2.4.2 fMRI data acquisition

fMRI data were acquired on a Philips 3.0 T Ingenia MR scanner (Philips Healthcare, Best, Netherlands) using a 32-element SENSE head coil. Data were collected using a gradient echo (GE) echo-planar imaging (EPI) acquisition at 1.5 mm isotropic spatial resolution, field of view (FOV) of 168 × 168 × 34.5 mm, echo time (TE) of 35 ms; flip angle = 90°; sensitivity encoding (SENSE) factor 2.5; and repetition time (TR) of 2 s. 23 coronal

172 oblique contiguous slices were acquired with equidistant temporal slice spacing and descending slice scan

173 order to provide coverage of the brainstem and Heschl's gyrus. To optimize placement of the FOV over the

174 ascending auditory pathway, a real-time functional localizer was used to map responses to eight repeats of a

175 24-s 10-Hz amplitude-modulated broadband noise stimulus followed by 40-s rest periods. This was followed

176 by collection of four 10-minute fMRI runs, resulting in a total of 32 cycles (384 'sound on' volumes, and 800

177 'sound off' volumes) of the broadband noise block paradigm each participant. Breathing and cardiac

178 pulsatility was recorded throughout the fMRI acquisition using respiratory bellows and a peripheral pulse

179 unit attached to the index finger of the left hand (Philips Healthcare, Best, Netherlands) for correction of

180 respiratory and cardiac physiological noise.

181 Additional EPI volumes were acquired with reversal of the fat-shift direction for image distortion correction,

182 particularly important for alignment of group averaged brainstem fMRI (e.g. Guimaraes et al., 1998). For

183 accurate co-registration of the fMRI EPI data to standard MNI template space, a whole-brain 3D anatomical

184 MPRAGE (Magnetization Prepared Rapid Acquisition Gradient Echo; TE = 2.7 ms, TR = 5.9 ms, flip angle of 8°;

185 and FOV 168 × 168 × 164 mm with reconstructed voxel size 1.5 mm^3) was acquired with the same spatial

186 resolution and angulation as the GE-EPI fMRI data. In addition, a high-resolution 3D T$_2$-weighted Turbo Spin

187 Echo (TSE) anatomical image was acquired (sagittal, TE = 278 ms, TR = 2000 ms, flip angle of 90°; and FOV

188 249 × 249 × 72 mm with reconstructed voxel size 0.576 mm^3) on which to overlay the statistical maps.

189

190 ### 2.4.3 fMRI data pre-processing

191 Image pre-processing was performed using FSL software (version 6.0, FMRIB's Software Library, UK), SPM12

192 software (Wellcome Trust Centre for Neuroimaging, UK) and in-house software coded in MATLAB. For each

193 individual participant, the fMRI time-series was motion corrected in SPM12. GE-EPI data were then

194 distortion corrected using FSL's TOPUP algorithm (Andersson et al., 2003; Smith et al., 2004) and corrected

195 for physiological noise using the respiratory and cardiac traces in RETROICOR (Glover et al., 2000). Following

196 this, data were spatially smoothed using a Gaussian kernel of full-width half-maximum 2 mm. Binarized

197 masks of white matter and cerebrospinal fluid were formed from the MPRAGE image using the segmentation

198 tool in SPM12 and threshold at 0.99999. The mean timecourse of white matter and cerebrospinal fluid (CSF)

199 signal within these masks was used as covariates in the general linear model (GLM).

200

201 ### 2.4.4 Efficacy of the fMRI preprocessing pipeline

202 As an adjunct to the main research question, we performed a post-hoc interim analysis on a subset of the

203 first 25 participants recruited to the study (9F/16M, aged 31.0 ± 3.9 years) to determine whether the fMRI

204 statistical maps of the sustained fMRI responses (which show greater activity for the auditory brainstem and

205 midbrain structures) were improved by distortion correction and physiological (cardiac and respiratory)

206 noise correction pre-processing steps. Spherical 6-mm ROIs were placed in the CN, SOC, NLL, IC and MGB

207 centered on co-ordinates previously specified by Gutschalk and Steinmann (2015), and the voxel with peak

208 sustained activity in the primary auditory cortex. Within these ROIs, sound-related fMRI responses that were

209 sustained over the 24-s on epoch were examined using a paired t-test to determine the combined effect of

210 the pre-processing steps. Random effects analyses were performed on spatially smoothed data analyzed

211 both without ('standard' pipeline) and with ('optimized' pipeline) distortion and physiological noise

212 correction. Both standard and optimized pre-processing pipelines detected robust sustained group-level

213 fMRI responses throughout the ascending auditory pathway (Figure 2). The optimized pre-processing yielded

214 a statistically significant improvement ($p < 0.05$) in the ability to detect group-level sound-related fMRI

215 responses in the NLL, MGB, and AC ROIs, and no detrimental effect in any region (Figure 2), so these two

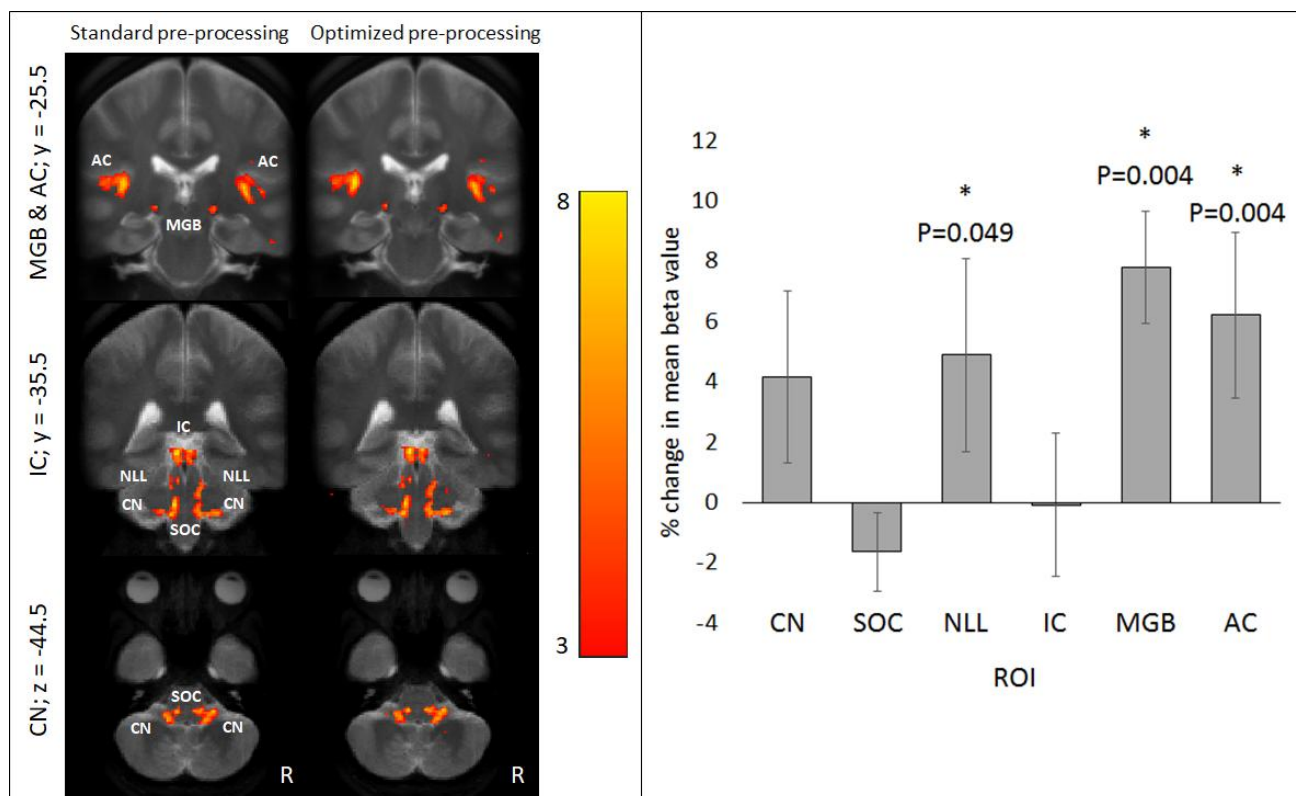216 pre-processing steps were applied to the full study.

Figure 2: Interim analysis of the influence of distortion and physiological noise correction on sound related activity in the ascending auditory pathway. Left: Group-level (n = 25) sustained sound-related activation for "standard" versus "optimized" pre-processing (p < 0.001 uncorrected, k = 0 voxels) overlaid onto the group-level mean T_2 turbo-spin echo image. 'y' and 'z' values denote the MNI slice co-ordinates of the coronal (top) and axial (bottom) images and the color bar denotes T statistic. Right: Group-level mean (± standard error) percent difference in beta values within spherical ROIs calculated for optimized (distortion correction and physiological noise correction) compared to standard pre-processing. A significant increase in beta value (* denotes p < 0.05) is evident in the NLL, MGB and AC ROIs.

Since there have been limited functional studies of subcortical regions, we also evaluated how sample size influences the ability to reliably detect subcortical auditory group responses. To address this, the number of participants used in the sustained response GLM was reduced to 25, 20, 15 and 10, and this result is shown as Supplementary data Table 1S.

232 **_2.4.5 fMRI data analysis_**

233 fMRI data were analyzed using a random effects GLM (SPM12) computed using successive first- and second-

234 level analyses. The design matrix in the first-level analysis defined the explanatory variables for each

235 individual participant and comprised the (i) transient phasic onset and offset stimulus responses, (ii)

236 sustained stimulus response, (iii) six motion parameters, and (iv) mean white matter and CSF signal time-

237 courses. In this GLM, the phasic responses were encoded as a series of delta functions and the sustained

238 response was encoded as a box-car function, and these were convolved with the hemodynamic response.

239 The phasic and sustained regressors were assessed for orthogonality, and a high degree of orthogonality was

240 found between the onset and offset regressors (-0.08), and onset/offset and sustained regressors (0.11 for

241 both onset/offset). Explanatory variables (iii) and (iv) were considered 'nuisance' variables (i.e. potential

242 confounds in the MR signal). The fMRI time-series was high-pass filtered to 1/128 Hz (twice the cycle length)

243 and modeled for temporal autocorrelation across scans with an AR(1) process. Contrast images

244 corresponding to stimulus onset, stimulus offset and the sustained response were generated for each

245 participant. The fMRI response to a continuous stimulus that is perceived as a single event has been shown

246 to vary systematically throughout the auditory pathway from one that is sustained over the stimulus epoch

247 (CN, SOC, NLL, and IC) to one that is phasic with transient peaks at stimulus onset and offset (MGB, auditory

248 cortex) (Gutschalk et al., 2010). This has been interpreted as representing a population neural

249 representation of the beginning and the end of distinct perceptual events that, while weak or absent in the

250 midbrain, begins to emerge in the thalamus and is robust in the auditory cortex. These different auditory

251 response characteristics informed two independent, yet complementary, analyses: i) a second-level voxel-

252 wise analysis of the fMRI contrast images to determine the effect of lifetime noise exposure within individual

253 auditory brain regions, and ii) mixed analysis of covariance (ANCOVA) to determine the effects of lifetime

254 noise exposure across ROIs within the ascending auditory pathway.

255 Each participant's MPRAGE image was transformed to the MNI template space in SPM12 (note: the fMRI

256 data was acquired at the same resolution and orientation as the MPRAGE image). This transform computes a

257 matrix for each participant's MPRAGE image using parameters that best align the template (tissue

258   probability map/atlas) to the individual participant's image using an affine registration (local optimization)

259   including regularization (penalizing excessive stretching or shrinking) to the MNI symmetric average brain

260   stereotaxic registration model. Following this, the transform was then applied to all contrast images for that

261   participant to move all data into MNI template space. Mean T_2 TSE maps were then computed by separately

262   co-registering each subject's T_2 TSE image to MNI space (the T_2 TSE images had a different resolution,

263   orientation and FOV to the fMRI data) before averaging across the group.

264   As described in the protocol (Dewey et al., 2018a), individual contrast images were combined in the second-

265   level GLM of the beta value of the auditory response (representing the magnitude of the stimulus fMRI

266   response) and noise exposure group as a between-subject factor. Voxel-wise statistical significance is

267   reported at $p < 0.05$ after small volume correction in *a priori* cortical and subcortical ROIs (see Section 2.4.6).

268   In addition, the individual contrast images were interrogated to quantify the average beta value within each

269   ROI on an individual participant basis. To address the primary hypothesis of increased responses in central

270   auditory regions in high lifetime noise exposure compared to low noise exposure, an ANCOVA was

271   performed, with the average beta values in each auditory region and hemisphere as within-subjects factors,

272   noise exposure (low, high) as a between-subjects factor, and de-meaned age as a covariate. Our defined

273   boundary of 15 units of noise exposure, corresponding to the NIOSH distinction between 'acceptable' versus

274   'at risk' noise exposure (National Institute for Occupational Safety and Health, 1998), allows for a high vs.

275   low group effect to be studied in noise exposure which itself is a continuous variable. Since the beta values

276   from the two GLMs (onset and sustained) are distinct dependent variables, these measures were used in

277   separate ANCOVAs (note this is a deviation from the protocol paper, in which we stated that responses

278   would be used as levels of a within-subjects factor analysis, which is not a valid statistical analysis).

279   In an exploratory investigation to examine the association between sound-related activity and noise

280   exposure, a GLM was performed on individual contrast images (both for onset and sustained responses)

281   using noise exposure as a continuous linear regressor, with de-meaned age as a regressor of no interest.

282   Further GLMs were also estimated to address exploratory research questions; these included either tinnitus

283   (present, absent) or reduced sound-level tolerance (present, absent) as the between-subjects factor instead

284   of noise exposure group.

285

286   ### 2.4.6 Region of interest (ROI) definition

287   Use of anatomical landmarks or manual segmentation is challenging for auditory brainstem and midbrain

288   ROIs (Devlin et al., 2006). Instead, a region of interest (ROI) analysis to quantify activity in anatomically

289   defined areas specified in template volume space was performed following the method used by Gutschalk

290   and Steinmann (2015). Subcortical nuclei were determined based on macroscopic anatomy of the average

291   brain, in combination with cross reference to the co-ordinates previously specified by Gutschalk and

292   Steinmann and the contrast images obtained for the 'sound on versus sound off' contrast. Auditory cortex

293   was similarly defined using the anatomical boundaries of Heschl's gyrus/gyri; the superior temporal gyrus

294   and the superior temporal sulcus located lateral and posterior to it, and the 'sound on versus sound off'

295   contrast. The 'sound on versus sound off' contrast was a summed composite (OR in Boolean algebra) of the

296   three binary images generated by thresholding ($p < 0.01$ corrected for family-wise error; FWE) the contrast

297   images for stimulus onset, stimulus offset and the sustained responses across all participants (n = 62).

298   Region-specific ROIs for CN, SOC, NLL, IC, MGB and auditory cortex were subsequently created from each

299   sub-region within this binary mask. These ROIs were then used to estimate activity in the subcortical and

300   cortical areas for each noise exposure group from the contrast images estimated in the first-level analysis for

301   each participant.

302

2.5 ABR assessment

The methodology for ABR assessment followed previous work by co-authors (Guest et al., 2017; Prendergast et al., 2017a).

2.5.1 Stimuli

ABR stimuli comprised single-polarity high-pass filtered clicks (using a first-order Butterworth filter with high-pass cut-off of 1.4 kHz) presented at 102 dB peak equivalent SPL. Stimuli were generated using in-house software written in MATLAB (version 2016a, The MathWorks Inc.). Stimuli were presented via shielded Etymotic (Etymotic Research, Inc., Elk Grove Village, Illinois) ER3A transducers with disposable insert foam ear tips. Stimulus presentation was alternated between ears at a rate of 22 Hz (11 Hz per ear) for a total of 7000 clicks per ear.

2.5.2 ABR data acquisition

Electrical activity was recorded using the BioSemi ActiveTwo multichannel electroencephalography (EEG) system with active electrodes (BioSemi BV, Amsterdam, Netherlands). Three channels were used with electrodes attached to the vertex/Cz, right mastoid and left mastoid with 10/20 electrode paste. Two additional electrodes were attached to the forehead (< 3 inches apart) to form the ground (Common Mode Sense and Driven Right Leg). Recording was performed in an electrically shielded, darkened, soundproof room, whilst participants lay flat. Participants were instructed to close their eyes, relax, and feel free to fall asleep if able to. Stimuli were presented near-continuously throughout an initial relaxation period prior to recording. Recording commenced when the EEG trace had stabilized, and motion artefacts had subsided. The recording lasted approximately 10 minutes.

2.5.3 ABR data analysis

ABR data were processed using in-house software coded in MATLAB (Guest et al., 2017; Dewey et al., 2018b). For each participant and for each ear, the time-course of the potential difference between Cz and the ipsilateral mastoid was divided into epochs extending from 10 ms pre-stimulus to 13 ms post-stimulus, after correcting for the 0.91 ms acoustic delay introduced by the tube connecting the transducer to the ear. Epochs with a root-mean-square amplitude of more than 2 standard deviations above the mean were rejected. Data were then averaged across trials, again separately for left and right ear stimulus presentations, and the resulting averaged waveforms were filtered using a fourth-order Butterworth filter between 50 Hz and 1.5 kHz. Filtered averaged waveforms were then baseline-corrected by subtracting the mean amplitude of the 2 ms preceding arrival of the stimulus at the ear drum.

Amplitudes of the peak of ABR waves I and V were quantified to address the primary hypothesis of difference in responses between the low and high noise exposure groups. In addition, the amplitude ratio of waves I/V was computed to provide within-subject normalization and reduce inter-individual variation (Schaette and McAlpine, 2011). Wave I and wave V peaks were identified automatically, using an algorithm that picked out features of the ABR waveform in pre-defined time windows. Peak-picking windows were adjusted slightly from those specified in the protocol, based on observed peak latencies in our cohort (latencies used to develop the protocol were obtained using slightly different methods and equipment). Thus, the peak of wave I was defined as a local maximum falling 1.5 to 2.5 ms after the calculated arrival time of the stimulus at the ear. If no maximum existed within this window, then the peak of wave I was defined as the highest point within the window. The trough of wave I was defined as the lowest point between 0.3 and 0.8 ms following the wave I peak. The peak of wave V was defined as a local maximum falling between 5.3 and 6.6 ms after the arrival of the stimulus. There were four exceptions (out of 124 ears) where it was necessary to deviate from these rules by altering the time windows in order to successfully characterize one of the peaks: three participants displayed a short wave I, so the relative window for identifying the trough of wave I was between 0.2 and 0.6; one participant exhibited an unusually late wave V so the time window for identification was extended to 7.1 ms after the arrival of the stimulus. To assess any

Page 19

352 effect of lifetime noise exposure on either ABR wave I or V amplitudes or on wave I/V amplitude ratio, mixed

353 ANCOVA models were specified with noise exposure (low, high) and sex as between-subject factors, and the

354 de-meaned age as a covariate (Van Breukelen and Van Dijk, 2007). Two further ANCOVA models were

355 specified with different between-subjects factors representing (presence/absence of) tinnitus and

356 (presence/absence of) sound-level tolerance.

357

358 **3. Results**

359 **3.1 Participant characteristics**

	Low Noise Exposure	High Noise Exposure
Number	30	32
Sex (F/M)	12/18	9/23
Age in years (mean± st.dev; median; range)	32.0 ± 4.5; 31.0; 25-40	32.0 ± 4.5; 32.5; 25-40
Lifetime noise exposure in units of energy (mean ± st.dev, median, range)	4.0 ± 3.5; 3.6; 0-14	45.0 ± 37.3; 31.0; 15-189
Presence of tinnitus	6	13
Presence of reduced sound-level tolerance	6	10
Presence of hearing problems	13	22
Tinnitus intrusiveness (mean ± st.dev, median, range)	1.2 ± 3.2; 0.0; 0-15	1.9 ± 2.8; 0.0; 0-9

360

361 **Table 1**: Baseline characteristics of the low and high noise exposure groups. Descriptive statistics of the

362 tinnitus and sound-level tolerance scores are across all individuals including those with a score of 0. Scores

363 on the tinnitus intrusiveness scale range from 0 to 30.

364

365   Table 1 summarizes the characteristics of the low and high noise exposure groups. All age subgroups

366   comprised at least six participants, with the 28-30 and 31-33 year subgroups each comprising seven

367   participants in the high noise exposure group. Comparison of the baseline characteristics between low and

368   high noise exposure groups found no statistically significant differences in sex (X^2_1(N = 62) = 3.663, p = 0.056,

369   Table 1) nor audiometric thresholds from 0.25 to 16 kHz ($F_{1,60}$ = 0.100; p = 0.752). These observations at 12

370   and 16 kHz ($F_{1,60}$ = 0.166; p = 0.685) indicate balanced high-frequency hearing sensitivity (Figure 3, individual

371   thresholds shown in Figure 1S of Supplementary data). Audiometric thresholds at 16 kHz could not be

372   measured in those ears in which thresholds exceeded 90 dB HL since the output level of the equipment was

373   limited to this value, and as such were recorded as 90 dB HL for reporting. This accounted for 6 out of 60

374   ears in the low noise exposure group and 4 out of 64 ears in the high noise exposure group. Although there

375   was an overall trend towards higher thresholds at 4 kHz, in individual participants this dip was too shallow to

376   be defined as a noise-induced (notched) hearing loss (McBride and Williams, 2001). Reports of tinnitus and

377   reduced sound-level tolerance using the THS were more common in the high noise exposure group than low

378   (X^2_1(N = 62) = 5.963, p = 0.015 and X^2_1(N = 62) = 7.650, p = 0.006, respectively), with tinnitus perceived as

379   more intrusive in the high noise exposure group (Mann-Whitney U = 359.5, median = 0.0, p = 0.037) (Table

380   1). However, tinnitus intrusiveness scores were low and would not be interpreted as clinically indicative for

381   either group. Six participants in the high noise exposure group and two in the low noise group experienced

382   both tinnitus and reduced sound level tolerance. Hearing problems as reported in THS responses were

383   equally common across both groups (X^2_1(N = 62) = 2.517, p = 0.113, Table 1).
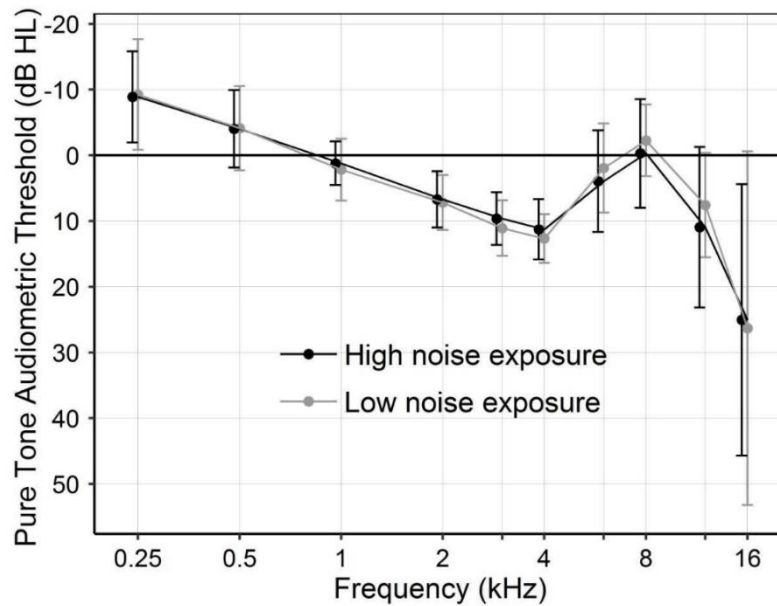
384

385

Figure 3: Audiometric threshold (lines denote means and error bars denote standard deviations) over 250 Hz to 16 kHz for low and high exposure groups. Thresholds ≤ 20 dB HL over the range 500 Hz to 8 kHz were amongst the eligibility criteria for inclusion in the study. 4/60 [low noise exposure group] and 7/64 [high noise exposure group] participants were not measured at 16 kHz as their audiometric thresholds were > 90 dB HL (greater than the output level of the audiometer) and as such their 16 kHz values were recorded as 90 dB HL.

392

393 3.2 fMRI responses
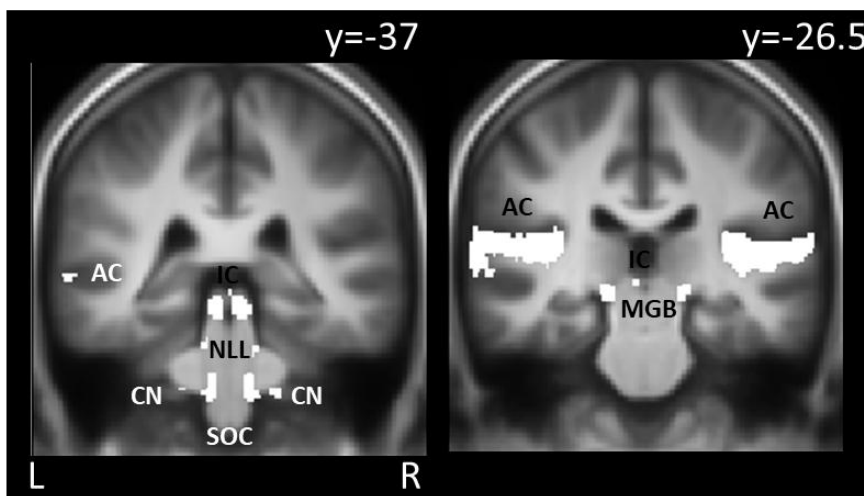
ROI	Size of ROI	
	Left	Right
AC	1,424	1,921
MGB	22	37
IC	82	80
NLL	10	8
SOC	53	57
CN	85	67

394

Figure 4: Left: Illustrative coronal slices showing the ascending auditory pathway ROIs as defined from the 'OR' combination of binary masks generated from the random effects GLMs of the onset, offset and sustained responses of all (n = 62) participants at p < 0.01 family-wise error (FWE) corrected. ROIs are shown in the cochlear nucleus (CN), superior olivary complex (SOC), nucleus of the lateral lemniscus (NLL), inferior colliculus (IC), medial geniculate body (MGB) and auditory cortex (AC), and overlaid on the group-level mean MPRAGE image (L = left, R = right), 'y' denotes the MNI slice co-ordinates. Right: Number of voxels (1.5 mm isotropic) in each ROI by hemisphere.

3.2.1 Robust sound-related responses throughout the subcortical auditory pathway

Group (n = 62) data showed robust activation in response to the broadband noise stimulus. Figure 4 shows the subcortical and cortical ROIs generated. In agreement with previous reports (Giraud et al., 2000; Harms and Melcher, 2002; and a review article by Nourski and Brugge, 2011), the early ascending auditory pathways (CN and IC) responded predominantly with a sustained response, whilst the auditory cortex showed a strong phasic response to stimulus onset and offset (Figure 5). Our protocol pre-specified analysis of CN, IC, MGB and auditory cortex, but robust responses were additionally detected in the SOC and NLL, as shown by the ROI time-courses (Figure 5). Visual inspection shows that the onset of the phasic response is more sensitive to the stimulus features than the offset, particularly for the CN, IC and MGB (and additionally SOC, NLL; Figures 6 and 7) and that the sustained regressor is a poor match to the shape of the BOLD response in the auditory cortex compared to subcortical regions
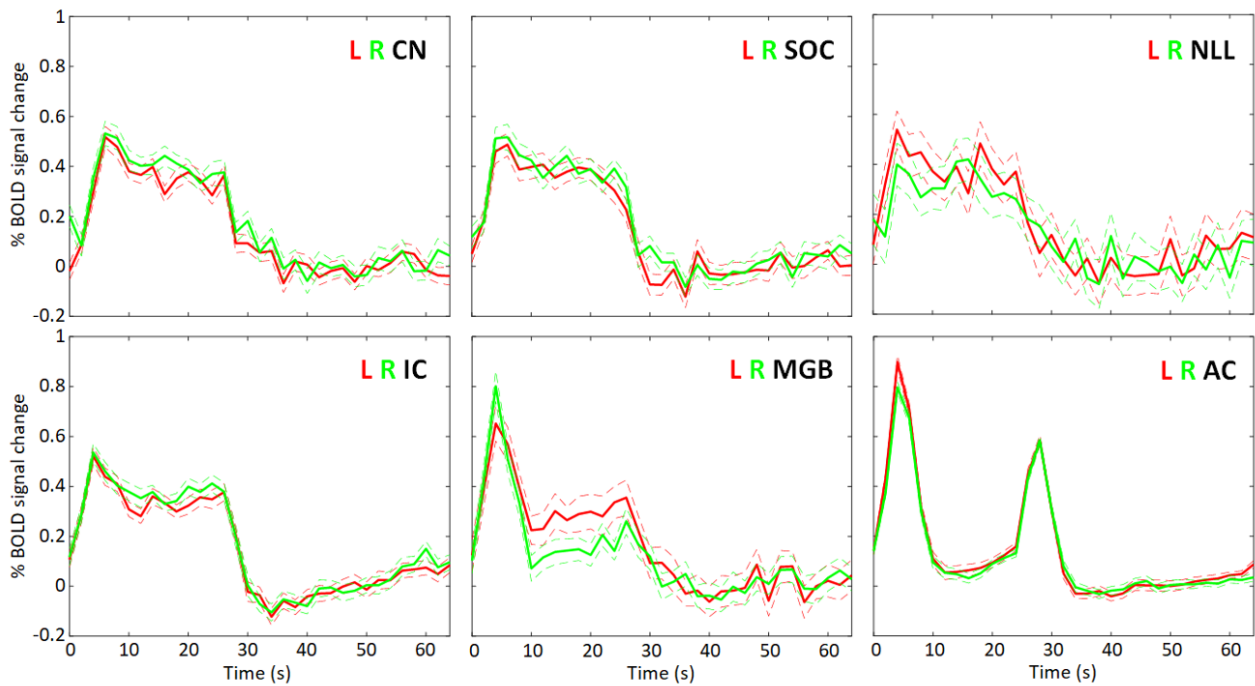
Page 23

Figure 5: Group mean BOLD percentage change to broadband noise stimulation (all participants, n = 62) in the CN, SOC, NLL, IC, MGB and auditory cortex (AC). Dashed lines show standard error. Note the systematic variation in the fMRI response to the broadband noise stimulus epoch throughout the auditory pathway from one that is sustained over the stimulus epoch (CN, SOC, NLL, and IC) to one that is phasic at stimulus onset and offset (MGB, AC).

3.2.2 Effect of noise exposure on transient auditory activity in the ascending auditory pathway

Voxel-wise analysis of the contrast images for the transient onset showed greater auditory activity in the high noise exposure group compared to the low noise exposure group, particularly in the right auditory cortex when corrected for multiple comparisons (FWE) at the cluster level ($p < 0.05$, see Figure 6). ANCOVA statistics on the ROI analysis showed that lifetime noise exposure is associated with a significant increase in the response to stimulus onset throughout the ascending pathway. An ANCOVA model with noise exposure and region (CN, IC, MGB, auditory cortex) as main factors, and de-meaned age as a covariate, showed that mean beta values were greater in the high than the low noise exposure groups ($F_{1,59} = 4.79$; $p = 0.033$) in addition to a significant effect of region ($F_{3,177} = 116.99$; $p < 0.001$), but no effect of hemisphere ($F_{1,59} = 0.74$;

431   p = 0.39). Although the response was greatest in auditory cortex, absence of an interaction between region

432   and noise exposure group (p = 0.39) suggests that the effect of lifetime noise exposure might not be limited

433   to auditory cortex. Including SOC and NLL as two additional regions in the ANCOVA model also gave a

434   significant noise exposure group effect. Note, ANCOVA analysis assumes that all mean beta values are

435   normally distributed, but assessment of kurtosis and skewness in individual ROIs indicated that this was not

436   the case for responses in bilateral CN (p < 0.01) (Field, 2009). All main effects and interactions were

437   confirmed when the CN data were removed, demonstrating that non-normality did not impact the result. An

438   exploratory analysis estimated the GLM using noise exposure as a linear continuous regressor and the

439   transient response as the dependent variable. No brain regions demonstrated a statistically significant linear

440   response. Voxel-wise offset responses were weaker than for the stimulus onset responses (see also Figure

441   5), and as such only the onset response was assessed.

442
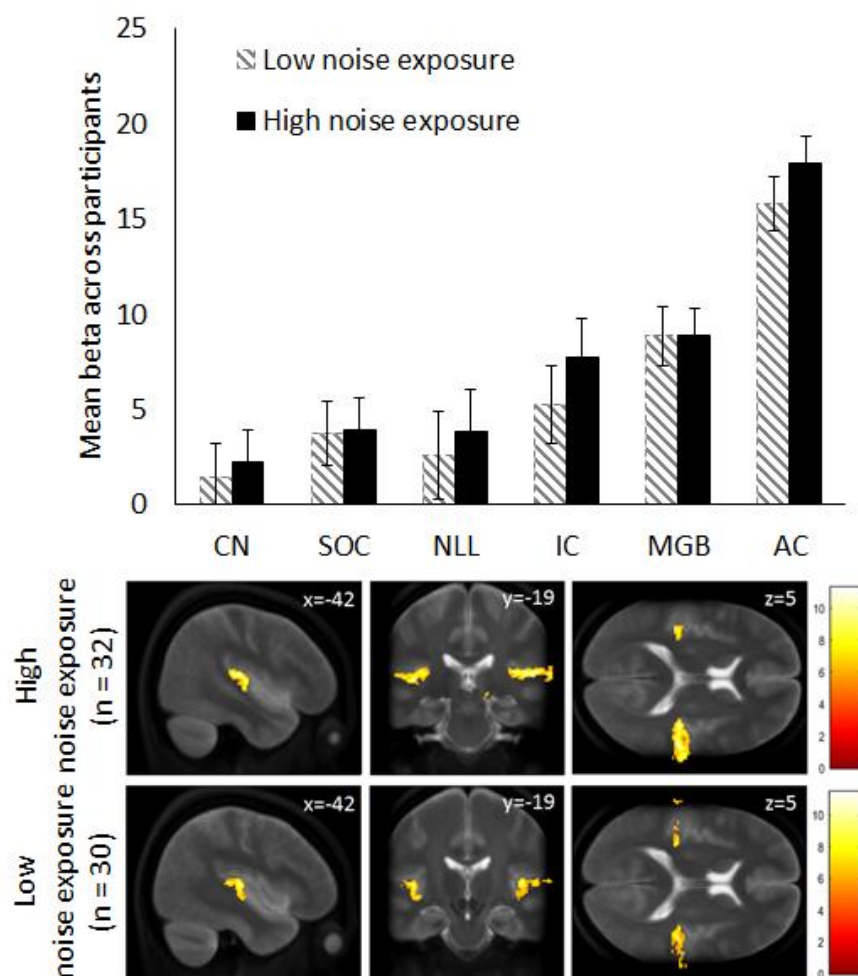
443   **Figure 6**: Onset response: estimated marginal mean ROI beta values for stimulus onset in ROIs in low and

444   high noise exposure groups. Beta values represent an average over left and right hemispheres, error bars

445   represent the 95% confidence intervals of the mean. Random effects group activations to the stimulus onset

446   for the low (n = 30) and high (n = 32) noise exposure groups threshold at $p < 0.05$ FWE corrected with the

447   color bar showing the T statistic. Numbers within the images denote co-ordinates of sagittal, coronal and

448   transverse slices. Statistical maps are overlaid on the mean (n = 62) T_2 TSE image.

449

450   ***3.2.3 Effect of noise exposure on sustained auditory activity in the ascending auditory pathway***

451   Voxel-wise analysis of the contrast images to quantify sustained activity again showed evidence for greater

452   auditory activity in the high noise exposure group than in the low noise exposure group in the right AC when

453   FWE corrected at the cluster level (Figure 7). An ANCOVA on the sustained response beta values in CN, IC,

454   MGB and auditory cortex ROIs (with all beta values being normally distributed, i.e. exhibiting no significant

455   skew or kurtosis at levels of $p < 0.01$) showed overall differences in the magnitude of the response across

456   ROIs ($F_{3,177} = 59.44$; $p < 0.001$), with the subcortical ROIs, specifically IC, showing the greatest response and

457   auditory cortex the smallest. However, for the sustained response there was a non-significant trend of noise

458   exposure group ($F_{1,59} = 3.63$; $p = 0.06$) and hemisphere ($F_{1,59} = 2.67$; $p = 0.11$), with no significant interaction

459   between region and noise exposure group ($p = 0.65$). As above for the transient responses, including SOC

460   and NLL as two additional regions gave the same pattern of results. Again, an exploratory analysis modelling

461   the effect of noise exposure as a linear continuous independent variable did not reveal any significant
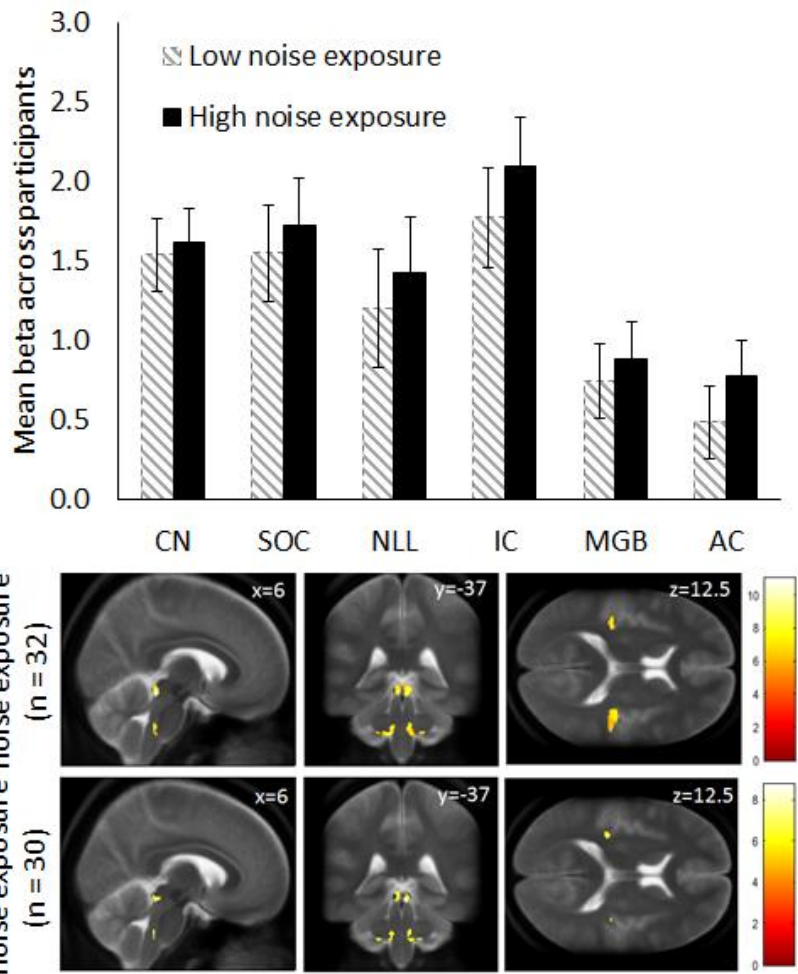
462   effects.

463

Figure 7: Sustained response: estimated marginal mean ROI beta values for sustained stimulus in ROIs in low

and high noise exposure groups. Beta values represent an average over left and right hemispheres, with

error bars representing 95% confidence intervals of the mean. Below: random effects group activations to

the sustained stimulus for low (n = 30) and high (n = 32) noise exposure groups threshold at $p < 0.05$ FWE

corrected with the color bar showing the T statistic. Numbers within the images denote co-ordinates of

sagittal, coronal and transverse slices. Statistical maps are overlaid on the mean (n = 62) T_2 TSE image.

470

471 ### *3.2.4 Effect of tinnitus and sound-level tolerance on sustained and transient ascending auditory pathway*

472 ### *function*

473 Exploratory ANCOVA models with tinnitus or sound-level tolerance as main factors in place of noise

474 exposure group demonstrated no main effect of tinnitus or sound-level tolerance on the sustained response

475 (tinnitus: $F_{1,59}$ = 0.003; p = 0.96; sound-level tolerance: $F_{1,59}$ = 0.25; p = 0.62), or on the onset response

476 (tinnitus: $F_{1,59}$ = 1.19; p = 0.28, sound-level tolerance: $F_{1,59}$ = 0.05; p = 0.83).
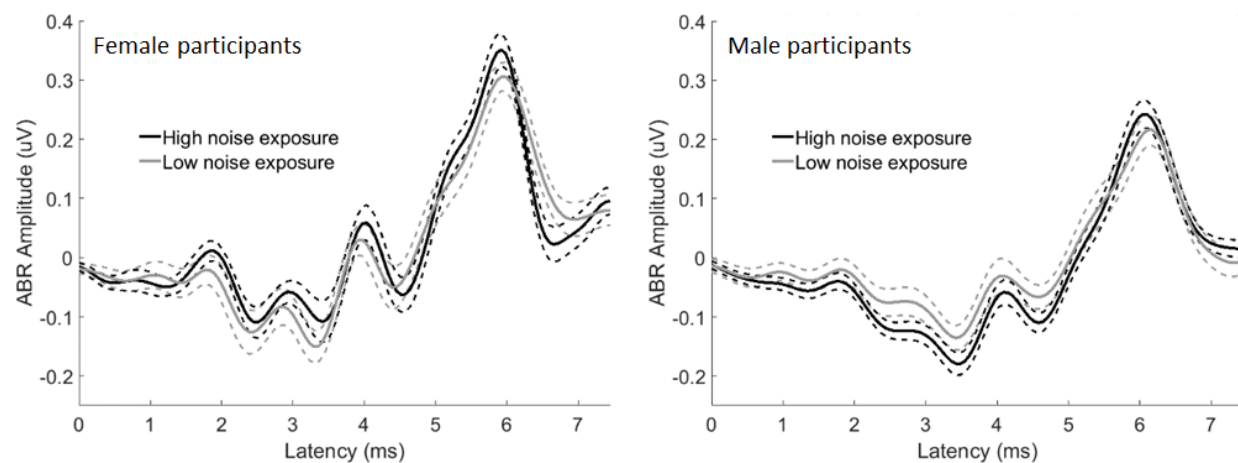
477

478 ## 3.3 ABR results

479

480 **Figure 8**: Group-level grand averaged ABR waveforms. Black lines denote the high noise exposure group (n =

481 32, nine female) and grey lines denote the low noise exposure group (n = 30, 12 female). Solid lines

482 represent the average and dashed lines represent the standard error. In both panels, the grand average was

483 created by first averaging across left and right ears within subjects, and then averaging across subjects.

484

485 Visual inspection of the group-level grand averaged waveforms confirmed a typical ABR profile (Figure 8).

486 There was no significant difference in the amplitudes of wave I and V between the left and right ears across

487 the participant group (ANCOVA $F_{1,61}$ = 0.127; p = 0.723) and no interaction between wave and ear ($F_{1,61}$ =

488 0.667; p = 0.417). Hence, all subsequent analyses used amplitude estimates averaged across ears.

489 ABR wave I and V amplitudes followed a normal distribution with no skewness or kurtosis (p > 0.01) (Field,

490 2009). There was no effect of noise exposure on ABR amplitude ($F_{1,57}$ = 0.456; p = 0.502), nor any effect of

491   tinnitus ($F_{1,57}$ = 2.667; p = 0.108) or sound-level tolerance ($F_{1,57}$ = 1.067; p = 0.306). ABR amplitudes were

492   larger in females than males for both wave I ($F_{1,57}$ = 8.89; p = 0.004) and wave V ($F_{1,57}$ = 14.03; p < 0.001),

493   which may result mainly from sex differences in cochlear mechanical dispersion (Don et al., 1993). There was

494   no interaction between sex and noise exposure group ($F_{1,57}$ = 0.660; p = 0.420). The ratio of wave I/V

495   amplitude was not normally distributed, with both skew and kurtosis (p < 0.001) (Field, 2009). A Mood's

496   median test was performed as a nonparametric alternative to assess the effect of noise exposure; this

497   revealed no significant difference (p = 0.81; X^2_1 = 0.06; median = 0.46).

498   A correlation analysis was run between the magnitude of the fMRI onset response in bilateral NLL (averaged

499   across hemispheres) and wave V of the ABR (averaged across ears), but this was not significant (Pearson's r =

500   0.139; p = 0.280; n = 62).

501

502   **4. Discussion**

503   This is the first auditory fMRI evaluation of synaptopathy in humans, here we tested the hypothesis that

504   higher lifetime noise exposure would lead to increased responses in central auditory regions compared to

505   lower noise exposure. fMRI of the ascending auditory pathway was performed in 62 individuals with strictly

506   normal hearing thresholds (≤ 20 dB HL) from 500 Hz to 8 kHz, allocated to two groups of low and high noise

507   exposure who widely varied in their individual lifetime noise exposures (0 - 14 vs. 15 - 189 units). Groups

508   were closely balanced for age (exhibiting the same means, standard deviations and ranges) and high-

509   frequency audiometric thresholds (up to 16 kHz). Although the effect is small, our findings demonstrate for

510   the first time a significant effect of noise exposure on the fMRI response to the onset of a sound stimulus in

511   listeners with apparently normal hearing. Responses throughout the auditory system were greater in

512   individuals with higher lifetime noise exposure levels than in controls with low lifetime noise exposure levels.

513   These enhanced responses to transient stimuli concur with previously published data from animal models of

514   noise exposure (Sheppard et al., 2017; Schrode et al., 2018; Sheppard et al., 2018). This finding is in

515   agreement with the central gain hypothesis, in which a reduction in neuronal input at the auditory periphery

516   is restored through central compensatory mechanisms (Schaette and McAlpine, 2011; Valderrama et al.,

517 2018), resulting in enhanced cortical responses to an auditory stimulus. The significance of the onset

518 responses has been corrected for multiple comparisons of ROIs, but not against the sustained responses

519 since these are research questions driven by separate hypotheses for their outcomes. These findings now

520 warrant further replication to confirm a more generalized effect.

521

522 ### 4.1 Comparisons with the published literature in humans

523 The ABR findings of this study are in agreement with the published ABR literature that does not report an

524 association between noise exposure and ABR waves I or V (Fulbright et al., 2017; Grinn et al., 2017;

525 Prendergast et al., 2017a), but contradicts Stamper and Johnson (2015b) who found an inverse relationship

526 between ABR wave I amplitudes and noise exposure, and Liberman et al. (2016) who found a positive

527 relationship between noise exposure and the ratio between waveform peaks generated by hair cells (the

528 summating potential to action potential ratio, SP/AP). Interestingly, in our fMRI responses we report a

529 positive relation between noise exposure and the physiological fMRI response, which is in-line with Liberman

530 et al. (2016). The disagreement between our ABR and fMRI findings may be due to electrophysiological

531 measures not being sensitive to subclinical noise-induced synaptopathy in humans, and the different origins

532 of the hemodynamic and electrophysiological signals.

533 The differences between our results and previously published studies may reflect methodological

534 differences. The present study measured audiometric thresholds at extended high frequencies of 12 kHz and

535 16 kHz, and as such is able to report that these thresholds did not significantly differ between noise exposure

536 groups. In contrast, Stamper and Johnson (2015a, b) compared audiometric thresholds between noise

537 exposure groups only up to 8 kHz, allowing a potential confound of high-frequency hearing loss between

538 groups. Further, Stamper and Johnson (2015b) used a noise exposure measure that reflected only exposures

539 over the previous year, whereas the present study used a lifetime noise exposure measure. The present

540 study did not have any hypothesis regarding sex of participants and the fMRI response, whereas conversely

541 there is a known relationship between ABR amplitudes and sex, and as such this was a confound in Stamper

542 and Johnson's original work, which was clarified in a subsequently published letter (Stamper and Johnson,

543 2015a).

544 The ABR performed in the present study used a click level of 102 dB peak equivalent SPL. As discussed in

545 Prendergast et al. (2017a), this may not have extensively stimulated all auditory nerve fibers with high

546 characteristic frequencies.

547 Similarly, some studies investigating associations between electrophysiological ABR measures and tinnitus

548 perception do report a positive association (Schaette and McAlpine, 2011; Gu et al., 2012; Bramhall, 2019),

549 whilst others (Guest et al., 2017; Shim et al., 2017) do not. The discrepancy between the present study and

550 the findings of Gu et al. (2012) may be attributed to the exploratory nature of the tinnitus question in the

551 present study and thus the lack of control for confounding factors across groups with and without tinnitus

552 (see Section 4.3).

553

554 *4.2 Considerations of fMRI and ABR findings*

555 The neural coding of stimulus onset is a more dominant feature within the central auditory pathway.

556 Therefore, while central gain might be expected to operate across both onset and sustained responses,

557 there might be greater sensitivity to detect central gain in the transient response. The group difference

558 between low and high noise exposure seen in cortical fMRI responses to stimulus onset ($p = 0.033$) is of the

559 same order as that observed by Gu et al. (2010) in individuals with reduced sound-level tolerance. This

560 positive fMRI finding counters the often null findings obtained to date using human ABR (Grinn et al., 2017;

561 Guest et al., 2017; Prendergast et al., 2017a), including those reported within this paper. While wave V of

562 the ABR represents activity in the NLL (Ponton et al., 1996), the magnitude of the fMRI onset response in NLL

563 and the amplitude of ABR wave V were not correlated. There are three putative explanations for these

564 results. First, it should be noted that the sample size was powered to detect a change in the fMRI response,

565 rather than ABR. Second, while the ABR directly measures a neuronal response, this is linked to the fMRI

566 signal through a chain of metabolic and hemodynamic processes. As ABR and fMRI measure two distinct

567 physiological phenomena, an effect seen in the hemodynamic response does not necessarily lead to the

568 same pattern in the neuronal response. Third, the data indicated that onset fMRI responses were largely

569 driven by AC activity.

570

571 ### 4.3 Limitations and future directions

572 There are several open questions that arise that require further confirmation. While it could be that all

573 significant noise-induced synaptopathy (regardless of susceptibility) is associated with audiometric losses, it

574 is also possible that susceptibility to noise damage is heterogeneous across the population, with some

575 individuals being more susceptible to noise exposure and others more resilient. Susceptible individuals may

576 be those for whom synaptopathy is masked by cochlear damage resulting in audiometric losses, and hence

577 they would not meet eligibility for inclusion in the present study. Such heterogeneity, if present, would

578 certainly reduce our sensitivity for detecting the central effects of noise exposure in participants with

579 clinically normal hearing.

580 It is currently unknown exactly what factors affect whether noise exposure does or doesn't lead to

581 synaptopathy in humans, indeed there remains a debate on the origin of hidden hearing loss in humans, and

582 the array of noise types inflicted on human listeners is vast. Consequently, the types of noise exposures

583 reported by participants in the present study varied across individuals. Some participants reported exposure

584 through listening to music (personal stereo, live music events) and others reported exposure to occupational

585 noise from machinery or transport noise, somewhat complicating interpretation of our results. However, this

586 is typical of the field (Xiong et al., 2014; Bramhall et al., 2017; Eggermont, 2017; Kobel et al., 2017;

587 Valderrama et al., 2018). It is possible that the type of noise exposure would affect the impact of noise

588 exposure on fMRI responses, but there is limited information at present about what spectrotemporal

589 features of a sound exposure have the greatest damaging impact on high-threshold auditory nerve fibers.

590 There is relatively recent animal data strongly suggesting that equal energy exposure produces similar

591 synapse loss across different exposure durations (Kujawa, 2019). Therefore, total energy of exposure is

592 thought to be key to inducing a given level of synaptopathy, i.e. the integral over exposure level and duration

593 can be compared directly between exposures of different types, supporting the use of NESI methodology in

Page 32

594 this study. Impulse noise exposure is known to differently affect auditory nerve fibers, as accounted for in

595 the NESI (Guest et al., 2018c) using kurtosis-correction (Goley et al., 2011), however the NESI does not apply

596 this in a more fine-grained way than differentiating firearm exposure from other exposure types. As such we

597 did not purposively enroll participants according to their dominant type of noise exposure. It is also the case

598 that there is a lack of knowledge about whether noise exposure affects onset or sustained fMRI responses in

599 a linear or non-linear manner, hence our exploratory correlation analysis.

600 While tinnitus and hyperacusis are both suggested to be associated with increased gain as measured using

601 fMRI from brainstem to cortex (Eggermont 2014), our study included too few participants reporting these

602 clinical symptoms to test this hypothesis with statistical rigor (tinnitus n = 19 and reduced sound-level

603 tolerance n = 16), and further study is needed in this area. In addition, our designation into these categories

604 was based on an indicative score obtained from a patient-reported screening test, not a clinical diagnosis.

605 According to the scores obtained using the TFI intrusiveness subscale, even those reporting a score indicative

606 of tinnitus did not appear to be strongly bothered by it and so this subgroup would not constitute clinically

607 significant tinnitus.

608 The choice of fMRI acquisition was influenced by hardware and software practicalities at the time of the

609 protocol development (Dewey et al., 2018a). We considered both a sparse or clustered-sparse acquisition

610 and continuous acquisition with noise cancellation (Langers et al., 2014; Dewey et al., 2018b), but the

611 continuous acquisition has the advantage of sampling the profile of the hemodynamic response function

612 over the duration of the sound stimulus (Figure 5), allowing clear definition and separation of stimulus onset

613 and sustained responses. At the time of the study design, the OptoActive Active Noise Cancellation (ANC)

614 system would not apply noise cancellation to a scanning protocol with a sparse or clustered-sparse

615 acquisition. Due to the relatively high spatial resolution (chosen to image the subcortical nuclei) the field of

616 view of the fMRI acquisition was limited to 34.5 mm in the slice direction, precluding any opportunity to

617 observe brain regions outside the temporal lobe, for example the salience network, which may have a

618 significant role in attention during the fMRI task (Damoiseaux et al., 2006). These practical limitations may

619 be overcome in future studies by the implementation of simultaneous multislice acquisitions.

Page 33

620 Finally, our study design may have introduced an inadvertent reduction in sensitivity through correlations

621 introduced between the ROI definition method and assessment of the effect of noise exposure through use

622 of the same stimulus condition in both statistical contrasts (Kriegeskorte et al., 2009). However, the ROI

623 locations were entirely independent of the effect of noise exposure and also based on anatomical

624 definitions. Moreover, there were practical comfort limitations which restricted the overall scanning time

625 and this obviated our ability to use a fully independent set of conditions to robustly define the ROIs. We

626 recommend that a future study could use the binary mask devised here for ROI definition (this is provided as

627 Supplementary data).

628

629 ### *4.4 Optimization of study design, image acquisition and image analysis to improve data quality*

630 We applied Active Noise Cancellation during continuous fMRI acquisition to significantly reduce the impact

631 of acoustic scanner noise. The fMRI protocol acquisition and analysis was optimized to study subcortical

632 auditory responses, with data collected at 1.5 mm isotropic resolution to sample subcortical nuclei, use of a

633 broadband stimulus, and analysis pre-processing steps including distortion correction to improve image

634 quality and normalization of the brainstem at the group level and RETROICOR physiological noise correction

635 to reduce cardiac and respiratory noise (Figure 2). Previous studies have used cardiac-gated acquisition in

636 combination with sparse fMRI sampling to study subcortical activity, however this considerably limits the

637 spatial coverage and temporal sampling of the data acquisition and consequently statistical power. For

638 example, Gu et al. (2010) were unable to show CN activation at $p < 0.01$ in the majority of individuals, and

639 Gutschalk and Steinmann (2015) state that "an exact separation of these nuclei is probably beyond the

640 capability of the method". Several further papers (Smits et al., 2007; Lanting et al., 2008; Lanting et al., 2014)

641 report that they were unable to perform fMRI in "subcortical areas, where the motion represents a practical

642 limit in imaging" (Slabu, 2010, pp. 302). Slabu (2010) state that "Because the MGB, CN and SOC were

643 insufficiently activated across subjects, the analysis was focused on the IC and AC".

644 Previous fMRI studies have attempted to measure subcortical activity to auditory stimulation. However

645 many studies report group sizes which are likely to be underpowered, thus only able to map activity in some,

646 but not all, of the auditory structures. For example, Slabu (2010) included 10 individuals, while Lanting et al.

647 included 22 (2008) and 29 individuals (2014), and Steinmann and Gutschalk (2012) studied 12 individuals.

648 We show the effect of sample size on the sensitivity to detect group level subcortical responses (see Table

649 1S, Supplementary data) while recruiting an adequately-powered sample to detect an effect of lifetime noise

650 exposure on the dependent variable. In this study, recruitment was stratified for age in each participant

651 group, with subgroups containing comparable numbers, as outlined prior to commencing the study (Dewey

652 et al., 2018a) and audiometric thresholds were strictly within the clinically normal range and balanced

653 between groups. The latter is often overlooked (Melcher et al., 2000; Melcher et al., 2009; Schaette and

654 McAlpine, 2011) and is critical when making comparisons between participant groups (see Guest et al.,

655 2018a for a discussion).

656

657 ## 5. Conclusions

658 In summary, this study evaluated ABR and fMRI of the ascending auditory pathway in low and high noise

659 exposure groups. The results suggest that sub-clinical changes resulting from noise exposure in listeners who

660 appear to have 'normal' hearing can be detected in humans using non-invasive fMRI optimized for studying

661 the ascending auditory pathways.

662

663 **References**

664 Andersson JL, Skare S, Ashburner J (2003) How to correct susceptibility distortions in spin-echo echo-planar

665   images: application to diffusion tensor imaging. NeuroImage 20:870-888.

666 Auerbach BD, Rodrigues PV, Salvi RJ (2014) Central gain control in tinnitus and hyperacusis. Frontiers in

667   neurology 5:206.

668 Bramhall N, Garnett McMillan, Frederick Gallun, and Dawn Konrad-Martin. (2019) Auditory Brainstem

669   Response Demonstrates That Reduced Peripheral Auditory Input Is Associated with Self-report of

670   Tinnitus. OSF Preprints.

671   Bramhall NF, Konrad-Martin D, McMillan GP, Griest SE (2017) Auditory Brainstem Response Altered in

672   Humans With Noise Exposure Despite Normal Outer Hair Cell Function. Ear and hearing 38:e1-e12.

673   Damoiseaux JS, Rombouts SA, Barkhof F, Scheltens P, Stam CJ, Smith SM, Beckmann CF (2006) Consistent

674   resting-state networks across healthy subjects. Proc Natl Acad Sci U S A 103:13848-13853.

675   Devlin JT, Sillery EL, Hall DA, Hobden P, Behrens TE, Nunes RG, Clare S, Matthews PM, Moore DR, Johansen-

676   Berg H (2006) Reliable identification of the auditory thalamus using multi-modal structural analyses.

677   NeuroImage 30:1112-1120.

678   Dewey RS, Hall DA, Guest H, Prendergast G, Plack CJ, Francis ST (2018a) The Physiological Bases of Hidden

679   Noise-Induced Hearing Loss: Protocol for a Functional Neuroimaging Study. JMIR research protocols

680   7:e79.

681   Dewey RS, Hall DA, Guest H, Prendergast G, Plack CJ, Francis ST (2018b) Optimising the detection of

682   subcortical auditory function using fMRI. In: International Society for Magnetic Resonance in

683   Medicine.

684   Di Stadio A, Dipietro L, Ricci G, Della Volpe A, Minni A, Greco A, de Vincentiis M, Ralli M (2018) Hearing Loss,

685   Tinnitus, Hyperacusis, and Diplacusis in Professional Musicians: A Systematic Review. International

686   journal of environmental research and public health 15.

687   Don M, Ponton CW, Eggermont JJ, Masuda A (1993) Gender differences in cochlear response time: an

688   explanation for gender amplitude differences in the unmasked auditory brain-stem response. The

689   Journal of the Acoustical Society of America 94:2135-2148.

690   Eggermont JJ (2017) Effects of long-term non-traumatic noise exposure on the adult central auditory system.

691   Hearing problems without hearing loss. Hear Res 352:12-22.

692   Ferguson MA, Tomlinson KB, Davis AC, Lutman ME (2019) A simple method to estimate noise levels in the

693   workplace based on self-reported speech communication effort in noise. International Journal of

694   Audiology 58:450-453.

695   Field A (2009) Discovering statistics using SPSS, Third edition Edition: Sage.

696　　Fulbright ANC, Le Prell CG, Griffiths SK, Lobarinas E (2017) Effects of Recreational Noise on Threshold and

697　　　　Suprathreshold Measures of Auditory Function. Seminars in hearing 38:298-318.

698　　Furman AC, Kujawa SG, Liberman MC (2013) Noise-induced cochlear neuropathy is selective for fibers with

699　　　　low spontaneous rates. Journal of neurophysiology 110:577-586.

700　　Giraud AL, Lorenzi C, Ashburner J, Wable J, Johnsrude I, Frackowiak R, Kleinschmidt A (2000) Representation

701　　　　of the temporal envelope of sounds in the human brain. Journal of neurophysiology 84:1588-1598.

702　　Glasner T, van der Vaart W (2009) Applications of calendar instruments in social surveys: a review. Quality &

703　　　　quantity 43:333-349.

704　　Glover GH, Li TQ, Ress D (2000) Image-based method for retrospective correction of physiological motion

705　　　　effects in fMRI: RETROICOR. Magnetic resonance in medicine 44:162-167.

706　　Goley GS, Song WJ, Kim JH (2011) Kurtosis corrected sound pressure level as a noise metric for risk

707　　　　assessment of occupational noises. The Journal of the Acoustical Society of America 129:1475-1481.

708　　Grinn SK, Wiseman KB, Baker JA, Le Prell CG (2017) Hidden Hearing Loss? No Effect of Common Recreational

709　　　　Noise Exposure on Cochlear Nerve Response Amplitude in Humans. Frontiers in neuroscience

710　　　　11:465.

711　　Grose JH, Buss E, Hall JW, 3rd (2017) Loud Music Exposure and Cochlear Synaptopathy in Young Adults:

712　　　　Isolated Auditory Brainstem Response Effects but No Perceptual Consequences. Trends in hearing

713　　　　21:2331216517737417.

714　　Gu JW, Herrmann BS, Levine RA, Melcher JR (2012) Brainstem auditory evoked potentials suggest a role for

715　　　　the ventral cochlear nucleus in tinnitus. J Assoc Res Otolaryngol 13:819-833.

716　　Gu JW, Halpin CF, Nam EC, Levine RA, Melcher JR (2010) Tinnitus, diminished sound-level tolerance, and

717　　　　elevated auditory activity in humans with clinically normal hearing sensitivity. Journal of

718　　　　neurophysiology 104:3361-3370.

719　　Guest H, Munro KJ, Prendergast G, Howe S, Plack CJ (2017) Tinnitus with a normal audiogram: Relation to

720　　　　noise exposure but no evidence for cochlear synaptopathy. Hear Res 344:265-274.

Page 37

721   Guest H, Munro KJ, Prendergast G, Millman RE, Plack CJ (2018a) Impaired speech perception in noise with a

722   normal audiogram: No evidence for cochlear synaptopathy and no relation to lifetime noise

723   exposure. Hear Res 364:142-151.

724   Guest H, Plack CJ, Munro KJ, Hall DA, Dewey RS (2018b) The Noise Exposure Structured Interview (NESI): a

725   Comprehensive Self-Report Measure of Cumulative Lifetime Noise Exposure. In: Association for

726   Research in Otolaryngology.

727   Guest H, Dewey RS, Plack CJ, Couth S, Prendergast G, Bakay W, Hall DA (2018c) The Noise Exposure

728   Structured Interview (NESI): An Instrument for the Comprehensive Estimation of Lifetime Noise

729   Exposure. Trends in hearing 22:2331216518803213.

730   Guimaraes AR, Melcher JR, Talavage TM, Baker JR, Ledden P, Rosen BR, Kiang NY, Fullerton BC, Weisskoff RM

731   (1998) Imaging subcortical auditory activity in humans. Human brain mapping 6:33-41.

732   Gutschalk A, Steinmann I (2015) Stimulus dependence of contralateral dominance in human auditory cortex.

733   Human brain mapping 36:883-896.

734   Gutschalk A, Hamalainen MS, Melcher JR (2010) BOLD responses in human auditory cortex are more closely

735   related to transient MEG responses than to sustained ones. Journal of neurophysiology 103:2015-

736   2026.

737   Harms MP, Melcher JR (2002) Sound repetition rate in the human auditory pathway: representations in the

738   waveshape and amplitude of fMRI activation. Journal of neurophysiology 88:1433-1450.

739   Henry J (2015) Tinnitus and Hearing Survey: A Screening Tool to Differentiate Bothersome Tinnitus From

740   Hearing Difficulties. American Journal of Audiology 24:66-77.

741   Hickox AE, Larsen E, Heinz MG, Shinobu L, Whitton JP (2017) Translational issues in cochlear synaptopathy.

742   Hear Res 349:164-171.

743   Kobel M, Le Prell CG, Liu J, Hawks JW, Bao J (2017) Noise-induced cochlear synaptopathy: Past findings and

744   future studies. Hear Res 349:148-154.

745   Kriegeskorte N, Simmons WK, Bellgowan PS, Baker CI (2009) Circular analysis in systems neuroscience: the

746   dangers of double dipping. Nature neuroscience 12:535-540.

747   Kujawa SG (2019) Noise-induced cochlear synaptopathy with and without sensory cell loss. International

748   Hearing Loss Conference; Niagara-on-the-Lake, Canada.

749   Kujawa SG, Liberman MC (2009) Adding insult to injury: cochlear nerve degeneration after "temporary"

750   noise-induced hearing loss. The Journal of neuroscience : the official journal of the Society for

751   Neuroscience 29:14077-14085.

752   Kumar UA, Ameenudin S, Sangamanatha AV (2012) Temporal and speech processing skills in normal hearing

753   individuals exposed to occupational noise. Noise Health 14:100-105.

754   Langers DR, Sanchez-Panchuelo RM, Francis ST, Krumbholz K, Hall DA (2014) Neuroimaging paradigms for

755   tonotopic mapping (II): the influence of acquisition protocol. NeuroImage 100:663-675.

756   Lanting CP, De Kleine E, Bartels H, Van Dijk P (2008) Functional imaging of unilateral tinnitus using fMRI. Acta

757   oto-laryngologica 128:415-421.

758   Lanting CP, de Kleine E, Langers DR, van Dijk P (2014) Unilateral tinnitus: changes in connectivity and

759   response lateralization measured with FMRI. PLoS One 9:e110704.

760   Liberman MC, Epstein MJ, Cleveland SS, Wang H, Maison SF (2016) Toward a Differential Diagnosis of Hidden

761   Hearing Loss in Humans. PLoS One 11:e0162726.

762   Lutman ME, Davis AC, Ferguson MA (2008) Epidemiological evidence for the effectiveness of the noise at

763   work regulations. In: HSE, Health and Safety Executive.

764   McBride D, Williams S (2001) Characteristics of the audiometric notch as a clinical sign of noise exposure.

765   Scandinavian audiology 30:106-111.

766   Meikle MB et al. (2012) The tinnitus functional index: development of a new clinical measure for chronic,

767   intrusive tinnitus. Ear and hearing 33:153-176.

768   Melcher JR, Sigalovsky IS, Guinan JJ, Jr., Levine RA (2000) Lateralized tinnitus studied with functional

769   magnetic resonance imaging: abnormal inferior colliculus activation. Journal of neurophysiology

770   83:1058-1072.

771   Melcher JR, Levine RA, Bergevin C, Norris B (2009) The auditory midbrain of people with tinnitus: abnormal

772   sound-evoked activity revisited. Hear Res 257:63-74.

773 National Institute for Occupational Safety and Health NIOSH (1998) Occupational Noise Exposure. Criteria

774   For A Recommended Standard, US Department of Health and Human Services, Public Health Service,

775   Centers for Disease Control and Prevention, National Instiure for Occupational Safety and Health,

776   USA.

777 Nichols TE, Das S, Eickhoff SB, Evans AC, Glatard T, Hanke M, Kriegeskorte N, Milham MP, Poldrack RA, Poline

778   J-B, Proal E, Thirion B, Van Essen DC, White T, Yeo BTT (2017) Best Practices in Data Analysis and

779   Sharing in Neuroimaging using MRI. Nat Neurosci 20:299-303.

780 Nourski KV, Brugge JF (2011) Representation of temporal sound features in the human auditory cortex.

781   Reviews in the neurosciences 22:187-203.

782 Ponton CW, Moore JK, Eggermont JJ (1996) Auditory brain stem response generation by parallel pathways:

783   differential maturation of axonal conduction time and synaptic transmission. Ear and hearing

784   17:402-410.

785 Prendergast G, Guest H, Munro KJ, Kluk K, Leger A, Hall DA, Heinz MG, Plack CJ (2017a) Effects of noise

786   exposure on young adults with normal audiograms I: Electrophysiology. Hear Res 344:68-81.

787 Prendergast G, Millman RE, Guest H, Munro KJ, Kluk K, Dewey RS, Hall DA, Heinz MG, Plack CJ (2017b) Effects

788   of noise exposure on young adults with normal audiograms II: Behavioral measures. Hear Res

789   356:74-86.

790 Schaette R, McAlpine D (2011) Tinnitus with a normal audiogram: physiological evidence for hidden hearing

791   loss and computational model. The Journal of neuroscience : the official journal of the Society for

792   Neuroscience 31:13452-13457.

793 Schrode KM, Muniak MA, Kim YH, Lauer AM (2018) Central Compensation in Auditory Brainstem after

794   Damaging Noise Exposure. eNeuro 5.

795 Sheppard A, Liu X, Ding D, Salvi R (2018) Auditory central gain compensates for changes in cochlear output

796   after prolonged low-level noise exposure. Neuroscience letters 687:183-188.

797 Sheppard AM, Chen GD, Manohar S, Ding D, Hu BH, Sun W, Zhao J, Salvi R (2017) Prolonged low-level noise-

798   induced plasticity in the peripheral and central auditory system of rats. Neuroscience 359:159-171.

799 Shim HJ, An YH, Kim DH, Yoon JE, Yoon JH (2017) Comparisons of auditory brainstem response and sound

800   level tolerance in tinnitus ears and non-tinnitus ears in unilateral tinnitus patients with normal

801   audiograms. PLoS One 12:e0189157.

802 Slabu LM (2010) The effect of slice orientation on auditory FMRI at the level of the brainstem. Brain

803   topography 23:301-310.

804 Sliwinska-Kowalska M, Zaborowski K (2017) WHO Environmental Noise Guidelines for the European Region:

805   A Systematic Review on Environmental Noise and Permanent Hearing Loss and Tinnitus.

806   International journal of environmental research and public health 14.

807 Smith SM, Jenkinson M, Woolrich MW, Beckmann CF, Behrens TEJ, Johansen-Berg H, Bannister PR, De Luca

808   M, Drobnjak I, Flitney DE, Niazy RK, Saunders J, Vickers J, Zhang Y, De Stefano N, Brady JM, Matthews

809   PM (2004) Advances in functional and structural MR image analysis and implementation as FSL.

810   NeuroImage 23:S208-S219.

811 Stamper GC, Johnson TA (2015a) Letter to the Editor: Examination of Potential Sex Influences in . Auditory

812   Function in Normal-Hearing, Noise-Exposed Human Ears, Ear Hear, 36, 172-184. Ear and hearing

813   36:738-740.

814 Stamper GC, Johnson TA (2015b) Auditory function in normal-hearing, noise-exposed human ears. Ear and

815   hearing 36:172-184.

816 Steinmann I, Gutschalk A (2012) Sustained BOLD and theta activity in auditory cortex are related to slow

817   stimulus fluctuations rather than to pitch. Journal of neurophysiology 107:3458-3467.

818 Valderrama JT, Beach EF, Yeend I, Sharma M, Van Dun B, Dillon H (2018) Effects of lifetime noise exposure on

819   the middle-age human auditory brainstem response, tinnitus and speech-in-noise intelligibility. Hear

820   Res 365:36-48.

821 Van Breukelen GJ, Van Dijk KR (2007) Use of covariates in randomized controlled trials. Journal of the

822   International Neuropsychological Society 13:903-904.

823 World Health Organization WHO (1997) Prevention of Noise-Induced Hearing Loss. In: World Health

824   Organization, (WHO).

825   Xiong M, Yang C, Lai H, Wang J (2014) Impulse noise exposure in early adulthood accelerates age-related

826   hearing loss. European archives of oto-rhino-laryngology : official journal of the European Federation

827   of Oto-Rhino-Laryngological Societies (EUFOS) : affiliated with the German Society for Oto-Rhino-

828   Laryngology - Head and Neck Surgery 271:1351-1354.

829   Yeend I, Beach EF, Sharma M, Dillon H (2017) The effects of noise exposure and musical training on

830   suprathreshold auditory processing and speech perception in noise. Hear Res 353:224-236.

831   Young ED, Barta PE (1986) Rate responses of auditory nerve fibers to tones in noise near masked threshold.

832   The Journal of the Acoustical Society of America 79:426-442.

833   Zhao F, Stephens D (2007) A critical review of King-Kopetzky syndrome: Hearing difficulties, but normal

834   hearing? Audiological Medicine 5:119-124.

835